Therapeutic prostate cancer interventions

a systematic review on pubic arch interference and needle positioning errors

Bloemberg, Jette; de Vries, Martijn; van Riel, Luigi A.M.J.G.; de Reijke, Theo M.; Sakes, Aimée; Breedveld, Paul; van den Dobbelsteen, John J.

DOI
10.1080/17434440.2024.2374761

Publication date
2024

Document Version
Final published version

Published in
Expert Review of Medical Devices

Citation (APA)
Bloemberg, J., de Vries, M., van Riel, L. A. M. J. G., de Reijke, T. M., Sakes, A., Breedveld, P., & van den Dobbelsteen, J. J. (2024). Therapeutic prostate cancer interventions: a systematic review on pubic arch interference and needle positioning errors. *Expert Review of Medical Devices*, *21*(7), 625-641. https://doi.org/10.1080/17434440.2024.2374761

Expert Review of Medical Devices

ISSN: (Print) (Online) Journal homepage: www.tandfonline.com/journals/ierd20

Therapeutic prostate cancer interventions: a systematic review on pubic arch interference and needle positioning errors

Jette Bloemberg, Martijn de Vries, Luigi A. M. J. G. van Riel, Theo M. de Reijke, Aimée Sakes, Paul Breedveld & John J. van den Dobbelsteen

To cite this article: Jette Bloemberg, Martijn de Vries, Luigi A. M. J. G. van Riel, Theo M. de Reijke, Aimée Sakes, Paul Breedveld & John J. van den Dobbelsteen (23 Jul 2024): Therapeutic prostate cancer interventions: a systematic review on pubic arch interference and needle positioning errors, Expert Review of Medical Devices, DOI: 10.1080/17434440.2024.2374761

To link to this article: https://doi.org/10.1080/17434440.2024.2374761

EXPERT REVIEW OF MEDICAL DEVICES
https://doi.org/10.1080/17434440.2024.2374761

Taylor & Francis
Taylor & Francis Group

REVIEW

Therapeutic prostate cancer interventions: a systematic review on pubic arch interference and needle positioning errors

Jette Bloemberg [a*], Martijn de Vries[a*], Luigi A. M. J. G. van Riel [b], Theo M. de Reijke[b], Aimée Sakes[a], Paul Breedveld[a] and John J. van den Dobbelsteen[a]

[a]Department of Biomechanical Engineering, Faculty of Mechanical Engineering, Delft University of Technology, Delft, The Netherlands; [b]Department of Urology, Amsterdam University Medical Centers, University of Amsterdam, Amsterdam, The Netherlands

ABSTRACT

Introduction: This study focuses on the quantification of and current guidelines on the hazards related to needle positioning in prostate cancer treatment: (1) access restrictions to the prostate gland by the pubic arch, so-called Pubic Arch Interference (PAI) and (2) needle positioning errors. Next, we propose solution strategies to mitigate these hazards.

Methods: The literature search was executed in the Embase, Medline ALL, Web of Science Core Collection*, and Cochrane Central Register of Controlled Trials databases.

Results: The literature search resulted in 50 included articles. PAI was reported in patients with various prostate volumes. The level of reported PAI varied between 0 and 22.3 mm, depending on the patient's position and the measuring method. Low-Dose-Rate Brachytherapy induced the largest reported misplacement errors, especially in the cranio-caudal direction (up to 10 mm) and the largest displacement errors were reported for High-Dose-Rate Brachytherapy in the cranio-caudal direction (up to 47 mm), generally increasing over time.

Conclusions: Current clinical guidelines related to prostate volume, needle positioning accuracy, and maximum allowable PAI are ambiguous, and compliance in the clinical setting differs between institutions. Solutions, such as steerable needles, assist in mitigating the hazards and potentially allow the physician to proceed with the procedure.

This systematic review was performed in accordance with the PRISMA guidelines. The review was registered at Protocols.io (DOI: dx.doi.org/10.17504/protocols.io.6qpvr89eplmk/v1).

ARTICLE HISTORY
Received 26 March 2024
Accepted 27 June 2024

KEYWORDS
Brachytherapy; needle positioning error; prostate cancer; pubic arch interference; focal therapy; steerable needle

1. Introduction

1.1. Background

Prostate cancer is the second most-diagnosed cancer in men and was the fifth leading cause of cancer-related deaths worldwide in 2020 [1]. In the United States, prostate cancer was estimated to be the most-diagnosed cancer in men and the second leading cause of cancer-related deaths in 2023 [2]. When detected in an early and localized stage, treatments such as radical prostatectomy [3], external beam radiation therapy [4], or brachytherapy [5] can be performed. These are whole-gland treatment modalities and provide high rates of oncological control. This is at risk of negative side effects for the patient, such as irritative micturition, urinary incontinence, erectile dysfunction, and rectal toxicity, thereby lowering the Quality of Life (QoL) [6,7].

Over the past decade, a trend toward focal (boost) therapies has been observed that can potentially minimize negative side effects [6–8]. For example, brachytherapy is often used as a whole-gland monotherapy, but it can be used as a focal (boost) therapy as well. Brachytherapy modalities include Low-Dose-Rate Brachytherapy (LDR BT), High-Dose-Rate Brachytherapy (HDR BT), and Pulsed-Dose-Rate Brachytherapy (PDR BT), in which radioactive sources or catheters loaded with radioactive sources are placed in the prostate for irradiation. In LDR BT, the implanted radioactive sources are left permanently within the prostate. Whereas in HDR BT and PDR BT, the radioactive sources are temporarily placed into the prostate via needles or catheters. Focal boost therapies such as brachytherapy treat the tumor with high dosages of for example radiation, whilst the remainder of the prostate gland is treated with a lower dose. Focal therapy is a shift from whole-gland treatment to targeting the tumor, while sparing the surrounding healthy tissue, thereby preserving genitourinary and gastrointestinal function [9]. Focal treatment modalities include e.g. brachytherapy, Focal Laser Ablation (FLA), irreversible electroporation, cryotherapy, high-intensity focused ultrasound, and photodynamic therapy. These are percutaneous procedures in which needles are guided through the perineal skin to reach the target volume for treatment. However, potential perturbations while passing intermediate structures may cause hazardous situations. This study provides an overview of the

CONTACT Jette Bloemberg J.Bloemberg@tudelft.nl Bio-Inspired Technology Group, Faculty of Mechanical Engineering, Delft University of Technology, Mekelweg 2, Delft 2628 CD, The Netherlands
*These authors contributed equally to this work.

Supplemental data for this article can be accessed online at https://doi.org/10.1080/17434440.2024.2374761.

Article highlights

- Needle positioning errors can cause a suboptimal prostate cancer treatment.
- Excessive pubic arch interference can result in patient exclusion.
- Guidelines for needle positioning errors and pubic arch interference are ambiguous.
- The largest needle positioning errors are reported along the needle direction.
- Steerable needles might mitigate the hazards related to needle positioning.

quantification of these hazards and the associated current guidelines, and solution strategies to mitigate these hazards.

1.2. Hazards in needle positioning

Two hazards, widely reported in literature, can hamper adequate needle positioning. First, the pubic arch can restrict access to the ventrolateral part of the prostate. This affects the total needle geometry (i.e. the spatial composition of all inserted needles) in the target volume [10] as depicted in Figure 1(a), assuming currently available, rigid needles are inserted parallel to each other in the horizontal direction. This phenomenon is known as Pubic Arch Interference (PAI). Accessibility of all regions inside the target volume is a requirement in focal (boost) therapies and brachytherapy as whole-gland monotherapy to obtain homogeneity of the total needle geometry and to ensure an effective treatment [14]. The level of PAI indicates to what extent a homogeneous needle distribution can be achieved.

Secondly, needle positioning errors can arise from misplacement (i.e. the needle is positioned in a location different from the planned location due to unwanted needle deflections [15]) or needle displacement (i.e. the needle is shifted to a different location after positioning). Erroneous individual needle positioning induces treatment of unintended areas (Figure 1(b)), which might lead to undertreatment of tumor tissue or overtreatment of healthy tissue (e.g. urethra, bladder, rectum, and neurovascular bundle), leading to similar side effects as documented for whole-gland treatment modalities, such as irritative micturition, urinary incontinence, erectile dysfunction, and rectal toxicity, thereby lowering the QoL [6,7].

In this study, the term 'hazard' is used to refer to potential sources of harm related to transperineal needle positioning. These hazards are in particular (1) access restrictions to the prostate gland, i.e. PAI and (2) needle positioning errors. Insight into the quantification of these hazards and solution strategies to mitigate them can provide information about the impact of different hazards and may give clues about how to minimize these hazards. To our knowledge, a systematic overview of the scientific literature on the quantification of the hazards related to transperineal needle positioning in prostate cancer treatments and their corresponding guidelines is not yet available. Here, we intend to fill this gap by providing a systematic overview of the quantification of these

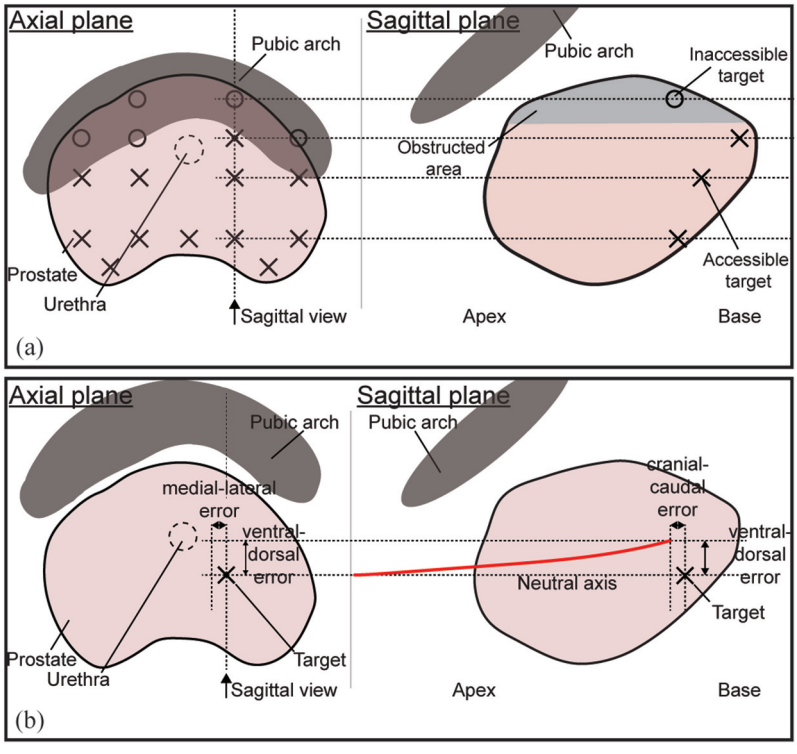

Figure 1. Hazards in needle positioning. (a) Schematic of total needle geometry in patients with Pubic Arch Interference (PAI). The planned total needle geometry, indicated in the axial plane, is based on the needle geometry of Mate et al. [11–13]. The pubic arch obstructs parts of the prostate resulting in a non-conformal total needle geometry, indicated by the light gray area in the sagittal plane, making accessible targets (X) inaccessible (O) using the transperineal approach with parallel horizontal needle trajectories (i.e. perpendicular to the transperineal template) using straight needle insertion. (b) Schematic of individual needle positioning errors in the prostate. The directions of the positioning error of the needle (red line) are shown in the axial and sagittal planes. The needle deviated from the neutral axis and did not reach the target (X).

hazards. Furthermore, we propose solution strategies to mitigate these hazards.

2. Methods

2.1. Scientific literature search

This systematic review was performed in accordance with the PRISMA guidelines. The review was registered at Protocols.io (DOI: dx.doi.org/10.17504/protocols.io.6qpvr89eplmk/v1). The literature search was executed using the Embase, Medline ALL, Web of Science Core Collection*, and Cochrane Central Register of Controlled Trials databases and included journal articles and conference abstracts in the English language. We used tailored search terms for each database using thesaurus terms (MeSH). The search keywords of the queries were organized into three categories: (a) therapy (e.g. brachytherapy, ablation therapy, laser ablation), (b) target (e.g. prostate, prostate tumor), and (c) needles and challenges or hazards (e.g. needle, catheter, probe, pubic). S1 Appendix shows the entire search queries for the used databases in this systematic review. The publication year for the conference abstracts was limited to 2019–2023.

2.2. Eligibility criteria

Throughout this review, the needle is defined as the device used to puncture tissues and position the energy or radiation source in the target volume. Only interventions were included with which prostate cancer can be treated locally via the transperineal pathway without resecting the prostate, excluding articles on diagnostics, treatment of benign tumors, (partial) resection of the prostate, and prostate volume determination. Regarding the study conditions, only clinical studies were accepted, whereas pre-clinical, phantom, animal, and simulation studies were excluded. Furthermore, only studies focused on the quantitative assessment of needle positioning were accepted, excluding studies solely focused on needle design, planning, patient selection, physician learning curve, automated needle detection, functional or biological outcomes, hospitalization time, and costs. Hazards unrelated to needle positioning were excluded, such as prostate movement due to bladder filling, brachytherapy seed migration, and inter-observer variability.

2.3. Literature search results

The search yielded 3309 articles (last update December 2023). Based on the eligibility criteria, two researchers (M.V. and J.B.) independently checked the titles, abstracts, and full texts subsequently in order to avoid bias. After full-text inspection, 50 articles were identified fulfilling all eligibility criteria (Figure 2). To our knowledge, no validated tool exists for assessing the risk of bias of studies on the quantification of PAI and needle positioning errors. Therefore, we created a series of six

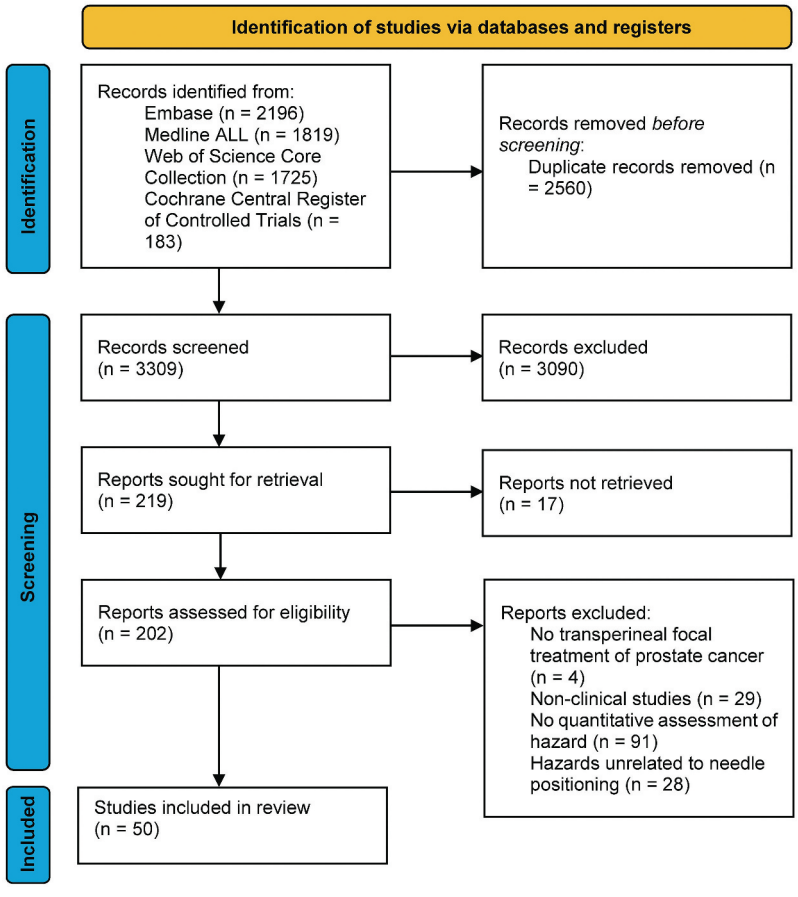

Figure 2. PRISMA flow diagram of the literature selection method.

parameters that can be used to orient the readers in making a judgment about the quality of the included studies (see S2 Appendix). The following data of the included articles were extracted: a) author name and year of publication, b) treatment type, c) number of patients, d) imaging modality, e) patient position during imaging, f) prostate volume, g) PAI or needle positioning errors measured, and h) time between implantation and error measurement.

3. Results

3.1. Quantification of hazards

3.1.1. Pubic arch interference (PAI)

PAI has been assessed in 15 included studies, as shown in Table 1. Eleven studies described the level of prostate obstruction by the pubic arch and fifteen studies reported the incidence of PAI for various prostate volumes. Sejpal et al. [22] researched the largest patient population, with 243 patients, and reported that 47 patients (19.3%) showed PAI during needle insertion.

PAI quantification is generally performed on Transrectal Ultrasound (TRUS)-Computed Tomography (CT) fusion imaging or Magnetic Resonance Imaging (MRI) scans, with the patient in supine position, whereas needle implantation is performed under Transrectal Ultrasound (TRUS) guidance with the patient in dorsal lithotomy position. Solely CT is less commonly used in clinical practice, due to its poor soft tissue contrast. The patient's position significantly influenced the level of observed PAI, ranging from 0 mm, if total clearance between the pubic arch and the prostate was observed, to 22.3 mm [22]. Tincher et al. [10] studied the level of PAI for seven patients after CT scans in both lithotomy and supine position. The authors reported that the patient's posture change from supine to lithotomy position decreased the level of PAI by 5 mm [10]. Next to posture change, the used imaging modality also induced discrepancies. Martin et al. [18] assessed PAI on TRUS, CT, and MRI scans. They found a linear correlation between PAI on the CT and MRI scans with the patient in supine position, whereas 75% of patients had larger values for PAI on CT compared to MRI. They reported PAI on CT and MRI of 2.9 ± 0.6 mm and 2.0 ± 0.6 mm (average ± standard error), respectively. PAI on the TRUS scans with the patient in lithotomy position was 0.6 ± 0.5 mm, which was different from both CT and MRI ($p < 0.06$). Strang et al. [25] reported that nine patients appeared to have PAI on CT, whereas only four of these nine patients had PAI on TRUS. The change in patients' posture from supine to lithotomy position and imaging modality reduced obstruction by the pubic arch by 11.8 mm on average. In contrast, Wallner et al. [28] showed a decrease of only 0.4 mm.

3.1.2. Needle positioning error

Thirty-five included studies documented quantitative needle positioning errors. Tables 2 and 3 show the reported misplacement and displacement errors, respectively. The majority of the studies (80%, 28/35) documented the error for an HDR BT treatment, 11% (4/35) for an LDR BT treatment, 6% (2/35) for a PDR BT treatment, and 3% (1/35) for an FLA treatment. The included studies reported needle misplacement and displacement assessed on anatomical images of the patient, but used different procedures and methodologies, such as (1) whether to change patient posture to allow for a specific imaging method and (2) varying imaging modalities, time intervals, and reference markers.

The patient's position regularly changed between the preoperative, intraoperative, and postoperative procedure [35–39], potentially influencing needle misplacement and displacement. Both Carrara et al. [40] and Cepek et al. [31] reported a single position (i.e. lithotomy position) for the entire duration of the procedure to minimize movement of the prostate and the tumor, and Cepek et al. [31] documented misplacement errors after needle insertions with symmetrical bevel-tip needles during FLA procedures of 1.1 mm, 1.8 mm, and 0 mm in the cranio-caudal, ventral-dorsal, and medial-lateral directions, respectively. They discussed that the error was caused mainly by needle deflection due to the initial skin puncture and the heterogeneity of tissue [31]. Carrara et al. [40] documented mean needle displacement of 0.8 and 0.0 mm in the ventral-dorsal and medial-lateral directions, respectively. In contrast, in the study by Buus et al. [41], patients were placed in supine position for the first MRI scan, in lithotomy position during implantation phase, and again in supine position for the second MRI scan to measure the error prior to treatment. The authors reported mean cranio-caudal needle displacements of 2.2 and 5.0 mm between the first and second HDR BT fraction and after the second HDR BT fraction, respectively. Another patient position transition was described by Mullokandov et al. [42]. In their study, the patients were taken out of the lithotomy position and placed in a frog-leg position (i.e. flexing the hips and abducting the legs) after implantation. The authors reported mean cranio-caudal needle displacements of 2 and 10 mm between the first and second HDR BT fraction and after the second HDR BT fraction, respectively.

Quantification of the error was performed using different imaging modalities, time intervals, and reference markers such as metal markers, bone anatomy, or other implanted needles [43,44]. Solely Smith et al. [45] measured the error along the entire needle length, whereas in other studies the end position of the distal tip was evaluated. Most studies used CT to measure the error (54%, 19/35), whereas some studies used X-ray (29%, 10/35), TRUS (20%, 7/35), MRI (11%, 4/35), or a combination of multiple imaging modalities (14%, 5/35). The time between the reference image and imaging after implantation ranged from nine minutes to four weeks.

Displacement errors were only reported for HDR BT and PDR BT. Most studies documented displacement in the cranio-caudal direction (i.e. 93%, 27/29), of which the largest average error of 20 mm was documented by Martinez et al. [46], who used 1.9-mm diameter flexible plastic needles with metal stylets during HDR BT. The authors stated that despite the needles being attached to the template, which was sutured to the perineal skin, the needles displaced up to 31 mm in the caudal direction [46]. They stated that the elasticity of perineal tissues was most likely the cause of needle displacement [46].

Pieters et al. [47] developed unique PDR BT catheters with an umbrella anchoring mechanism at the tip to fixate the catheter

Table 1. Overview of studies that evaluated pubic arch interference (PAI).

Level of PAI [mm]	Number of patients	Patients with PAI [%]	Imaging modality	Patient position	Prostate volume [cc]	Treatment	Authors
$\bar{x} = 9.5 \pm 6.9$ (0–22.3)	27	85.2	MRI	Supine	$\bar{x} = 92.3 \pm 38.0$ (48.0–178.9)	HDR BT	De Vries et al. [16]
(0–15.1)	40	25	MRI	Supine	$\bar{x} = 63.8 \pm 18.4$	LDR BT	Zheng et al. [17]
$\bar{x} = 2.0 \pm 0.6$ (0–12.5)	41	80.5	MRI	Supine		LDR BT	Martin et al. [18]
$\bar{x} = 2.9 \pm 0.6$ (0–12.5)	41	82.9	CT	Supine			
$\bar{x} = 0.6 \pm 0.5$ (0–4)	41	46.3	TRUS (5 mm)	Lithotomy	$\bar{x} = 32.6 \pm 2.3$		
(0 − > 5)	21	14.3	TRUS (5 mm)	Lithotomy	$\tilde{x} = 28.5$ $\bar{x} = 28.1$ (17.6–42.2)	LDR BT	Fukada et al. [19]
(0 − > 5)	21	28.6	CT (3 mm)	Lithotomy			
(0 − > 5)	21	23.8	CT + TRUS fusion	Lithotomy	$\tilde{x} = 29.5$ $\bar{x} = 28.8$ (19.0–39.9)		
(0–10)	5	100	TRUS (5 mm)	Lithotomy	<50 cc	LDR BT	Ryu et al. [20]
n/a	145	5.5	TRUS (7.5 MHz)	Lithotomy	$\bar{x} = 40.0$ (33.8–86.0)	LDR BT	Gibbons et al. [21]
$\tilde{x} = 6$ (0–10)	243	19.3	CT (5 mm)	Supine		LDR BT	Sejpal et al. [22]
	243		TRUS (5 mm)	Lithotomy	$\bar{x} = 44.7 \pm 11.1$*		
n/a	40	40	CT (5 mm)	n/a	$\bar{x} = 56 \pm 17$	LDR/HDR BT	Nickers et al. [23]
n/a	50	6	TRUS (7.5 MHz, 5 mm)	Lithotomy	$\bar{x} = 32$ (17–52)	LDR BT	Henderson et al. [24]
$\bar{x} = 12.2 \pm 3.4$ (8–20)	9	100	CT	Supine	$\bar{x} = 30.9 \pm 9.8$	LDR BT	Strang et al. [25]
$\bar{x} = 0.4 \pm 3.6$ (0–7)	14	28.6	TRUS (7 MHz, 5 mm)	Lithotomy	$\bar{x} = 39.0 \pm 18.1$		
$\bar{x} = 12.7$ (10–21)	7	100	CT (5 mm)	Supine	$\bar{x} = 34.6 \pm 11.4$ (17–48)	BT	Tincher et al. [10]
$\bar{x} = 7.8$ (6–12)	7	100	CT (5 mm)	Lithotomy			
(0–13)*	21	71.4*	CT (5 mm)	Supine		LDR BT	Wang et al. [26]
	33	n/a	TRUS (6 MHz, 5 mm)	Lithotomy	$\tilde{x} = 57$* (50–95)*		
$\tilde{x} = 0$ (0–20)	97	46.4*	CT (5 mm)	Supine		LDR BT	Bellon et al. [27]
	97		TRUS (6 MHz)	Lithotomy	$\tilde{x} = 36$ (15–131)		
$\bar{x} = 2.2 \pm 3.5$* (0–10)	16	62.5	CT (5 mm)	Supine		LDR BT	Wallner et al. [28]
$\bar{x} = 1.8 \pm 4.1$* (0–10)	16	50	TRUS (6 MHz)	Lithotomy	$\tilde{x} = 36$ (22–55)		
n/a	54	5.6	TRUS (4 or 5 MHz)	Lithotomy	≤60 cc	HDR BT	Borghede et al. [29]

For each study, the following information is reported: The level of PAI [mm], number of patients percentage of patients with PAI [%], imaging modality and patient position used for the assessment of prostate volume, prostate volume [cc], treatment, and reference. Clearance between the pubic arch and the prostate is reported as 0 mm PAI. $\tilde{x}$ = median, $\bar{x}$ = average ± standard deviation, and (.) = range.

BT = Brachytherapy, CT = Computed Tomography, HDR BT = High-Dose-Rate Brachytherapy, LDR BT = Low-Dose-Rate Brachytherapy, MRI = Magnetic Resonance Imaging, n/a = not available, TRUS = Transrectal Ultrasound, *If not specified in the manuscript, a best approximation was made based on the information in the graphs.

Table 2. Overview of studies that evaluated needle misplacement in transperineal prostate interventions.

Needle misplacement ± SD (range) [mm] (measurement method)								
Cranio-caudal	Ventral-dorsal	Medial-lateral	Number of patients	Imaging modality	Treatment	Patient posture change (pre-, intra-, postoperative)	Time [h]	Authors
$\bar{x}$ = 3.8 ± 0.2 (AM)	$\bar{x}$ = 1.5 ± 0.1 (AM)	$\bar{x}$ = 1.3 ± 0.1 (AM)	15	TRUS (6 MHz)	LDR BT	No change	n/a	Jamaluddin et al. [30]
$\tilde{x}$ = 1.1 (AM)	$\tilde{x}$ = 1.8 (AM)	$\tilde{x}$ = 0[a] (AM)	10	MRI (1.5T)	FLA, robotic implantation	No change	0.15	Cepek et al. [31]
n/a	>2 (MF)	>4 (MF)	5	TRUS (6.5 MHz), X-ray	LDR BT, robotic implantation	n/a	1	Fichtinger et al. [32]
n/a	$\bar{x}$ = 1.8 ± 0.6[b] (AM)	$\bar{x}$ = 1.8 ± 0.6[b] (AM)	30	TRUS (1 mm)	HDR BT	n/a	n/a	Szlag et al. [33]
n/a	$\tilde{x}$ = 3 (0–10)[b] (AM)	$\tilde{x}$ = 3 (0–10)[b] (AM)	10	MRI (0.5T)	LDR BT	No change	0.08–0.17	Cormack et al. [34]
$\bar{x}$ = 4.5 (IOF)	$\bar{x}$ = 2.2 (IOF)	$\bar{x}$ = 2.0 (IOF)	10	X-ray	LDR BT	n/a – lithotomy – supine	72	Taschereau et al. [15]

For each study, the following information is reported: Needle misplacement divided into cranio-caudal, ventral-dorsal, and medial-lateral directions, number of patients, imaging modality used for the assessment of misplacement, treatment, patient position pre-, intra-, and postoperatively, time between implantation and error measurement, and reference. $\tilde{x}$ = median, $\bar{x}$ = average ± standard deviation, and (,) = range.
MF = Marker Frames attached to needle guide, AM = Anatomical Marker (e.g. bone, urethra, ventral rectal wall, urethra, prostate base), FM = Fiducial Marker (e.g. gold maker), IOF = Isocentric Orthogonal Films, CT = Computed Tomography, FLA = Focal Laser Ablation, HDR BT = High-Dose-Rate Brachytherapy, LDR BT = Low-Dose-Rate Brachytherapy, MRI = Magnetic Resonance Imaging, n/a = not available or not applicable, TRUS = Transrectal Ultrasound, US = Ultrasound, [a]No statistically significant difference, no significant displacement, [b]Ventral-dorsal and medial-lateral errors were measured together as a single error.

inside the prostate gland. The authors stated that self-anchoring catheters showed an absolute mean displacement of 1 mm [47] compared to mean displacements of 11 to 13 mm in HDR BT of conventional needles [37,48,49]. The self-anchoring catheters were also used for HDR BT by Maenhout et al. [50], who reported an average three-dimensional (3D) error of 1.3 mm.

3.2. Clinical guidelines

Figure 3 provides a proposed decision-making process integrated into the current clinical workflow so that physicians can decide on the continuation of the procedure. This process includes published clinical guidelines retrieved from the included studies related to prostate volume, PAI, and needle positioning error. Exceeding a limit may result in patient exclusion or requires a solution to make the patient eligible again. In case of experiencing PAI during HDR or PDR BT treatment, one solution is to optimize the radiation dose by considering the actual positions of the implanted BT catheters. The radiation dose is determined by the dwell positions, i.e. the specific locations along the catheter where the radioactive sources reside, and the corresponding dwell times, i.e. the amount of time the radioactive sources reside at their dwell positions [51]. By increasing the dwell times of the catheters inserted as ventrally as possible and thus increasing the extension of the 100% isodose line, which defines the region where the radiation dose is equal to the prescribed dose, toward the ventral prostate areas, it becomes feasible to sufficiently irradiate the entire prostate also in case of PAI occurrence. However, a drawback is the potential creation of high-dose areas, which could impact nearby healthy Organs At Risk (OARs).

3.2.1. Prostate volume

Prostate volume is traditionally used as an indicator for the occurrence of PAI and is calculated on preoperative scans using the elliptical approximation: Prostate volume (cc) = π/6 (height x width x length) of the prostate [21]. The American Brachytherapy Society (ABS) guidelines state that focal (boost) treatment of a prostate volume of > 60 cc is technically more challenging as PAI is more prevalent in enlarged prostates. Thus, the ABS reported a prostate volume of > 60 cc as a relative contraindication for prostate brachytherapy [52]. In contrast, the revised Groupe Européen de Curiethérapie and the European SocieTy for Radiotherapy & Oncology (GEC-ESTRO) Advisory Committee for Radiation Oncology Practice (ACROP) prostate brachytherapy guidelines, published in 2022, state that a prostate gland of > 50–60 cc is no longer a contraindication for prostate brachytherapy as larger prostates can be successfully implanted if there is minimal PAI [53]. In some institutions, borderline cases with a prostate volume of 55 to 60 cc are generally better examined in accordance with the GEC-ESTRO ACROP guidelines. The prostate and the OARs are segmented on MRI or CT and digitally rotated to estimate the level of PAI in lithotomy position as described by de Vries et al. [22]. However, no guidelines are reported for

Table 3. Overview of studies that evaluated needle displacement in transperineal prostate interventions.

Needle displacement ± SD (range) [mm] (measurement method)										
Cranio-caudal			Ventral-dorsal	Medial-lateral						
<1 fraction	1–2 fraction	>2 fractions	<1 fraction	<1 fraction	Number of patients	Imaging modality	Treatment (number of fractions)	Patient posture change	Time [h]	Authors
$\bar{x} = 0.9 \pm 0.4$ (FM)	n/a	n/a	n/a	n/a	20	TRUS	HDR BT (1)	n/a	n/a	David et al. [95]
n/a	n/a	n/a	$\tilde{x} = 1.0$ (−1.7–1.8) (AM)	$\tilde{x} = 0.9$ (−0.9–1.5) (AM)	10	TRUS	HDR BT (1)	n/a	0.18	Wu et al. [96]
n/a	$\bar{x} = 2.2 \pm 1.8$ (IM)	$\bar{x} = 5.0 \pm 3.0$[d] (IM)	n/a	n/a	24	MRI (1.5T)	HDR BT (2)	Supine – lithotomy – supine	1–3	Buus et al. [41]
$\bar{x} = 3.8 \pm 3.2$ (FM)	n/a	n/a	n/a	$\bar{x} = 1.6 \pm 2.1$ (FM)	2	X-ray	HDR BT (2)	No change	0.25	Smith et al. [45]
n/a	$\bar{x} = 0.9$ (0–5.5) (during fraction) (AM)	n/a	$\bar{x} = 0.5$ (0–2.1) (during fraction) (AM)	$\bar{x} = 0.6$ (0–2.9) (during fraction) (AM)	17	MRI (1.5T)	HDR BT, self-anchoring catheter (1)	No change	n/a	Maenhout et al. [50]
n/a	n/a	n/a	$\bar{x} = 0.8 \pm 0.9$ (AM)	$\bar{x} = 0.0 \pm 1.8$ (AM)	14	TRUS (1 mm)	HDR BT (2)	No change	1–2	Carrara et al. [40]
n/a	(0–18)[c] (FM)		n/a	n/a	162	X-ray	HDR BT (4)	n/a	0–36	Aluwini et al. [57]
n/a	$\tilde{x} = 8.7 \pm 3.3$ (2.7 ± 1.1–14.7 ± 1.7) (FM)		n/a	n/a	20	CT (2 mm)	HDR BT (4)	n/a – lithotomy – supine	0–24	Reynés-Llompart et al. [39]
n/a	$\bar{x} = 0.97 \pm 0.76$[b] (FM)	n/a	$\bar{x} = 0.97 \pm 0.76$[b] (1–2 fraction) (FM)	$\bar{x} = 0.97 \pm 0.76$[b] (1–2 fraction) (FM)	33	CT (1 mm)	HDR BT (2)	n/a	6	Peddada et al. [97]
n/a	$\bar{x} = -0.22 \pm 0.2$[c] (FM)		$\bar{x} = -0.02 \pm 0.06$[c] (>1 fraction) (FM)	$\bar{x} = 0.01 \pm 0.04$[c] (>1 fraction) (FM)	23	CT (2 mm)	PDR BT, self-anchoring catheter (24)	n/a	2.2–48	Dinkla et al. [98]
$\bar{x} = 6 \pm 4$ (FM)	$\bar{x} = 12 \pm 6$ (FM)	$\bar{x} = 12 \pm 6$ (FM)	n/a	n/a	30	CT (1.25 mm)	HDR BT (5)	n/a	6–54	Kawakami et al. [99]
n/a	$\bar{x} = 5.8 \pm 1.9$ (−13–12) (FM, AM)	n/a	n/a	n/a	13	CT (2 mm)	HDR BT (3,4)	n/a – lithotomy – supine	0–48	Huang et al. [35]
n/a	$\bar{x} = 3.5$ (−14–13) (AM method) $\bar{x} = 2.3$ (−18–9) (FM method)	n/a	n/a	n/a	26	CT (1.25 mm)	HDR BT (1,2)	n/a – lithotomy – supine	36–672	Kovalchuk et al. [38]
n/a	$\bar{x} = 4.3 \pm 2.7$ (0.3–10) (FM)	$\bar{x} = 5.9 \pm 3.6$ (−2.3–12.9) (FM)	n/a	n/a	30	CT (3 mm)	HDR BT (7)	n/a	21–69	Takenaka et al. [62]
n/a	$\bar{x} = 5.1$ (1.9–10.1) (FM)	n/a	n/a	n/a	15	CT (3 mm)	HDR BT (2)	n/a	24	Foster et al. [100]
n/a	$\bar{x} = 12.6$ (0.6–24.6) (FM)	n/a	n/a	n/a	22	CT, X-ray	HDR BT (2)	n/a	24	Fox et al. [48]
$\bar{x} = 11.1 \pm 7.6$ (FM)	n/a	n/a	n/a	n/a	20	CT (3 mm, 1.5-mm interval), X-ray	HDR BT (1)	n/a – lithotomy – supine	2–3	Holly et al. [37]
0–0.5 (AM)	0–0.4 (AM)	n/a	0–1.3[a], 0–1.0[a] (1–2 fraction) (AM)	0–1.3[a], 0–1.0[a] (1–2 fraction) (AM)	25	TRUS	HDR BT (1)	n/a	0.83–1.2	Milickovic et al. [101]
$\tilde{x} = 7.5$ (−2.9–23.9) (FM)	n/a	n/a	n/a	n/a	25	CT (3 mm), X-ray	HDR BT (2)	n/a – lithotomy – supine	1.4–6.1	Whitaker et al. [36]

(*Continued*)

Table 3. (Continued).

Needle displacement ± SD (range) [mm] (measurement method)										
Cranio-caudal			Ventral-dorsal	Medial-lateral						
<1 fraction	1–2 fraction	>2 fractions	<1 fraction	<1 fraction	Number of patients	Imaging modality	Treatment (number of fractions)	Patient posture change	Time [h]	Authors
$\bar{x}$ = 4.5 ± 1.7 (FM)	$\bar{x}$ = 5.6 ± 3.6 (FM)	$\bar{x}$ = 6.4 ± 4.2 (FM)	n/a	n/a	91	CT (3 mm), X-ray	HDR BT (3)	n/a	0–48	Tiong et al. [58]
n/a	$\tilde{x}$ = 7 (−14–24) (FM)		n/a	n/a	64	CT (3 mm)	HDR BT (4,7,9)	n/a	72–120	Yoshida et al. [102]
n/a	$\bar{x}$ = 7.9 (0–21) (AM)	$\bar{x}$ = 3.8 (0–25.5) (AM)	n/a	n/a	20	CT (3 mm)	HDR BT (3)	n/a	21–28	Simnor et al. [63]
n/a	$\bar{x}$ = 2.7 (−6.0–13.5) (AM) $\bar{x}$ = 5.4 (−3.75–18.0) (FM)	n/a	n/a	n/a	10	CT (3 mm)	HDR BT (2)	n/a	24	Kim et al. [69]
$\bar{x}$ = 1.0 (0–6) (day 2), $\bar{x}$ = 1.2 (0–6) (day 3) (FM)			n/a	n/a	43	CT (2 mm)	PDR BT, self-anchoring catheter (46)	n/a	24–48	Pieters et al. [47]
n/a	$\bar{x}$ = 2 (0–4) (FM, AM)	$\bar{x}$ = 10 (5–23) (FM, AM)	n/a	n/a	50	CT (2 & 5 mm)	HDR BT (4)	n/a – lithotomy – frog-leg	3–28	Mullokandov et al. [42]
n/a	$\bar{x}$ = 11.5 (0–47) (IM)	n/a	n/a	n/a	20	CT (5 mm)	HDR BT (2)	n/a	18–24	Hoskin et al. [49]
n/a	$\bar{x}$ = 16 ± 6, $\tilde{x}$ = 18 (AM) $\bar{x}$ = 15 ± 4, $\tilde{x}$ = 12 (FM)		n/a	n/a	47	X-ray	HDR BT (4)	n/a	2–48	Pellizzon et al. [44]
n/a	$\bar{x}$ = 20 (FM, AM)	$\bar{x}$ = 4 (FM, AM)	n/a	n/a	10	TRUS (7.5 MHz, 5 mm), X-ray	HDR BT (4)	No change	6–36	Martinez et al. [46]
n/a	$\bar{x}$ = 6.8 (0–31.4) (FM) $\bar{x}$ = 8.3 (0–25.6) (AM)	$\bar{x}$ = 3.9 (0–10.4) (FM) $\bar{x}$ = 4.2 (0–9.1) (AM)	n/a	n/a	96	X-ray	HDR BT (4)	n/a	5–40	Damore et al. [43]

For each study, the following information is reported: Needle displacement in cranio-caudal direction before the first fraction, between the first and second fraction, and after the second fraction, needle displacement in ventral-dorsal and medial-lateral direction before the first fraction unless otherwise indicated, number of patients imaging modality, treatment, patient position pre-, intra-, and postoperatively, time between implantation and error measurement, reference. $\tilde{x}$ = median, $\bar{x}$ = average or mean, SD = Standard Deviation, and (.) = range.

AM = Anatomical Marker (e.g. bone, urethra, ventral rectal wall, urethra, prostate base), FM = Fiducial Marker (e.g. gold maker), IM = Ink Markers on the patient's skin or measurement of the needle outside the patient's body, CT = Computed Tomography, HDR BT = High-Dose-Rate Brachytherapy, MRI = Magnetic Resonance Imaging, n/a = not available or not applicable, PDR BT = Pulsed-Dose-Rate Brachytherapy, TRUS = Transrectal Ultrasound, [a]Ventral-dorsal and medial-lateral errors were measured together as a single error, [b]Cranio-caudal, ventral-dorsal, and medial-lateral errors were measured together as a single error, [c]Total error between all fractions was documented, [d]Total error between 1st and 3rd fractions were documented.

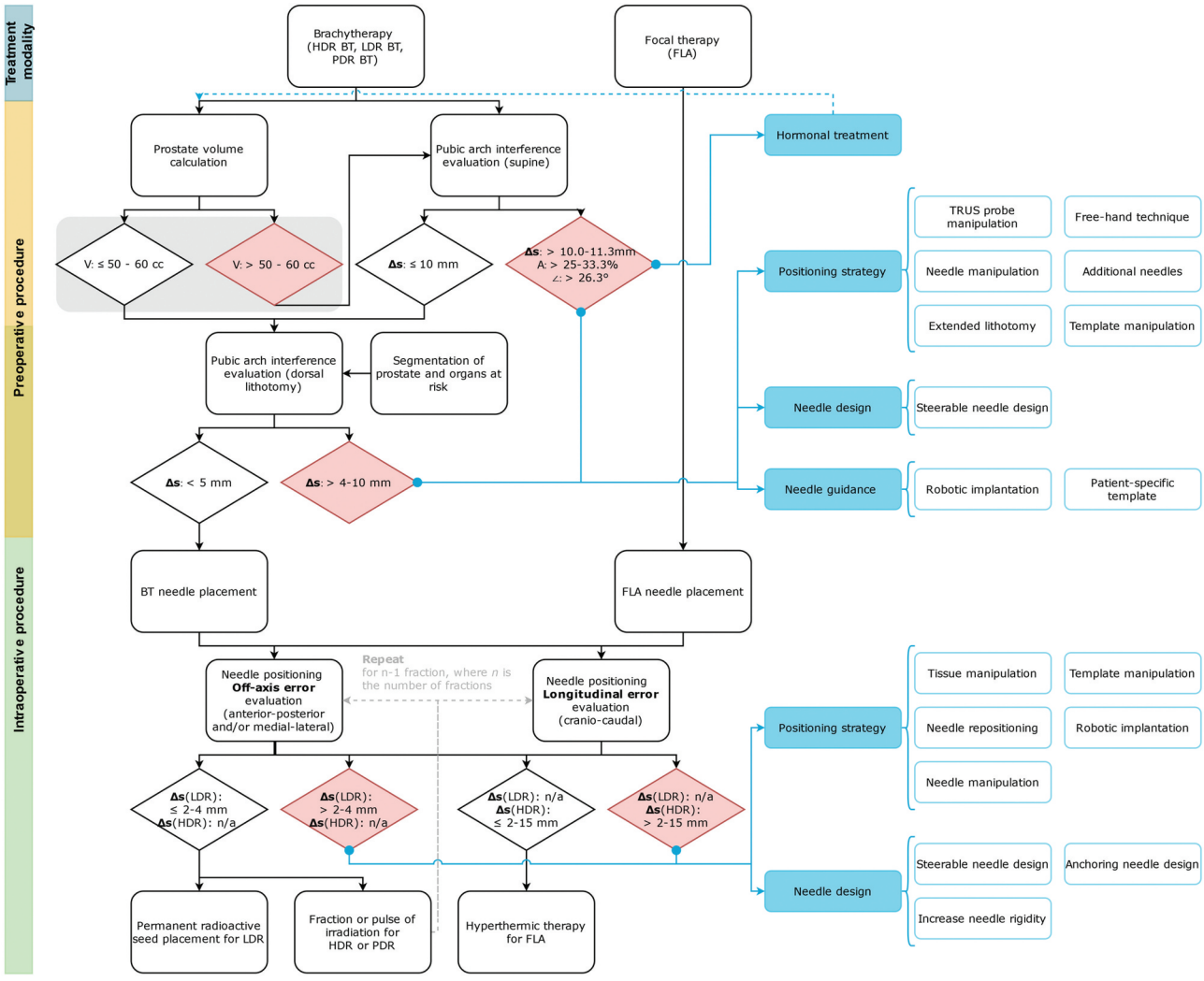

Figure 3. Decision-tree for conformity to treatment plan including clinical guidelines. Rounded rectangle shapes indicate procedural steps. Diamond shapes indicate the limits. Exceeding a limit (red diamond shape) requires a solution (blue rectangle shapes). Blue rectangle shapes indicate solutions for the procedural steps that the blue line with the dot grasps, the blue-outlined rectangle shapes indicate examples of the solutions. Note that the preoperative procedure (indicated in yellow) and the intraoperative procedure (indicated in green) partially overlap as the approaches differ between institutions. V = prostate volume, Δs = orthogonal distance from the inner surface of the pubic arch to the ventral border of the prostate in mm, a = obstructed area by the pubic arch compared to total prostate cross-section in %, ∠ = angle between the pubic symphysis and ventral border of the prostate. The gray block overlaid on the limits for prostate volume indicates that the guideline for prostate volume is superfluous according to new brachytherapy guidelines.

adequate rotation related to posture change from supine to lithotomy position.

3.2.2. Pubic arch interference

Prior to needle implantation, the level of PAI is measured on an MRI or CT scan with the patient in supine position to estimate the risk of obstruction during needle implantation with the patient in lithotomy position. Figure 4 indicates various methods to quantify PAI.

Firstly, the angle of PAI can be calculated in the sagittal plane by drawing two lines on the scan; one horizontal line through the pubic symphysis and one line connecting the most ventral point of the prostate with the most dorsal point of the pubic arch at the pubic symphysis (Figure 4(a)). Angle α between the pubic symphysis and ventral border of the prostate is the angle that can be related to a boundary value above which PAI is likely to occur. Zheng et al. [17] retrospectively analyzed MRI scans of 40 prostate cancer patients and suggested a boundary value of $\alpha = 26.3°$ to predict the occurrence of PAI in lithotomy position. They reported that the angle α of PAI was statistically correlated with the occurrence of PAI ($p < 0.01$).

Secondly, besides the angle of PAI, the distance of the obstruction between pubic arch and prostate can be assessed (Figure 4(b)). Multiple studies reported a threshold of 10.0 mm obstruction in supine position, assessed by overlaying the narrowest part of the pubic arch over the largest contour of the prostate in the axial plane and measured from the point of the prostate, which was at the greatest perpendicular distance from the caudal edge of the pubic arch [22,27]. Zheng et al. [17] suggested the boundary value of 11.3 mm as a reliable predictor of intraoperative PAI. They calculated PAI by using two parallel lines in sagittal plane through the pubic symphysis and reported a statistical correlation between distance and PAI ($p < 0.01$). When the distance exceeded 11.3 mm PAI was reported to be excessive.

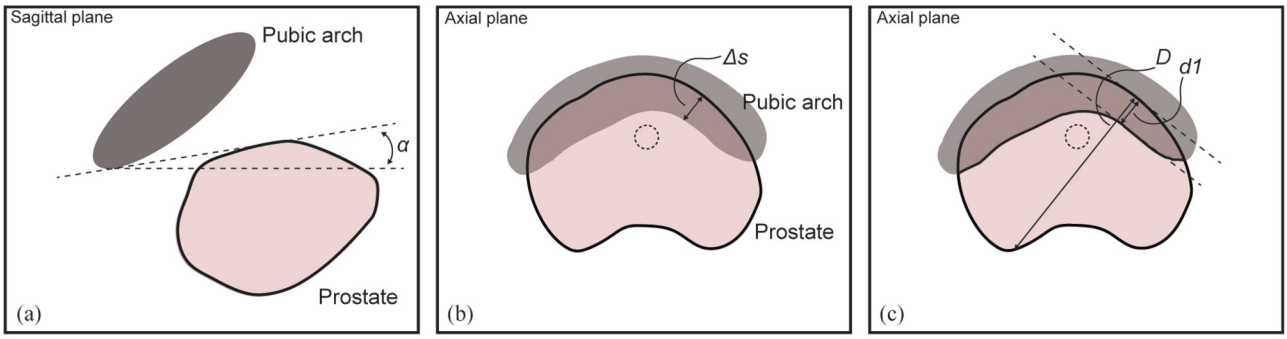

Figure 4. Measuring methods of pubic arch interference (PAI). (a) Angle (α) between pubic symphysis and ventral border of prostate, (b) Orthogonal distance (Δs) from inner surface of pubic arch to ventral border of the prostate and (c) Prostate diameter blockage (d1) by the pubic arch compared to total prostate diameter (D).

Lastly, Bellon et al. [27] and Henderson et al. [24] overlaid the largest prostate cross-section on the narrowest portion of the pubic arch. The percentage of overlapping prostate diameter indicates PAI (Figure 4(c)). Bellon et al. [27] and Henderson et al. [24] considered 25% and 33% obstruction of the prostate diameter in the axial plane as an indication of excessive PAI, respectively. These approximations were not based on a rigorous study. Some studies assessed PAI based on TRUS visualizations with the patient in lithotomy position. This position is associated with less PAI and larger accessibility of the prostate due to pelvic rotation than supine position [10]. Strang et al. [25] excluded patients with >4 mm PAI, whereas Fukada et al. [19] expected excessive PAI if >5 mm obstruction was shown, and Ryu et al. [20] excluded patients with >10 mm PAI.

3.2.3. Needle positioning error

Needle misplacement errors are affected by the needle-tissue interaction forces [54], needle design [55], and the implantation procedure [56]. On the other hand, needle displacement errors depend on the duration of treatment and perturbations between the needle positioning and treatment phase [48]. In HDR BT and PDR BT, the patient receives multiple treatment fractions, whereas in LDR BT and FLA, the patient receives a single dose. Multiple treatment fractions increase the time between needle positioning and treatment, which is associated with an increase in positioning error.

Several studies described correction of the needle position after the detection of misplacement or displacement. Aluwini et al. [57] reported that 43.8% of the HDR BT patients required at least one correction of the needle position of more than 3 mm, mostly in the cranial direction. Whitaker et al. [36] showed that 67% of the needles had a displacement in the cranio-caudal direction of at least 5 mm that required correction, and Tiong et al. [58] stated that up to three needles had to be corrected in cranio-caudal direction per fraction in HDR BT to lower the percentage of fractions from 82.3% to 12.2% in which displacements over 3 mm occurred. Buus et al. [41] reported that needle displacements of 3 and 5 mm introduced a decrease of 5 and 10% in target coverage for HDR BT, respectively. The authors proposed a 3D-positioning error threshold of 3 mm, calculated between HDR BT fractions, from the needle tip position relative to the corresponding transperineal template opening. For a single-fraction treatment with a dose of ≥15 Gy, they stated that displacement should be less than 2 mm due to the absence of the averaging dose effect of multiple fractions. Kolkman-Deurloo et al. [59] and Tiong et al. [58] analyzed the effect of needle displacements in HDR BT on X-ray scans along the longitudinal axis in simulation studies and recommended corrections of needles with an error exceeding 3 mm. It should be noted that the location of the needles in the transperineal template dictated the impact of the error on the OARs, as the needles in the dorsal rows were close to the rectum and the needles in the ventral rows were close to the urethra. Kolkman-Deurloo et al. [59] discussed that needles in the second and third dorsal rows of the transperineal template generally have larger impact on the dose coverage than needles in the ventral rows of the template because of the higher dwell weights (i.e. the relative contribution of a needle to the total administered dose in brachytherapy). Ventral rows of the template are less critical due to the lower dwell weights provided such that the dose to the urethra is not too high. Poder et al. [60] reported that 3D-source positioning errors in HDR BT plans could be up to 2 to 5 mm while avoiding significant (>10%) changes in the dose volume histogram of the prostate. Similarly, Mason et al. [61] investigated needle positioning errors and reported a threshold of approximately 2–3 mm based on a minimum value required for error detection and avoiding unnecessary countermeasures assessed by a physician. Nevertheless, the effect of the needle error still depended on the location of the needle in the target volume, the direction of the positioning error, and the weights of the dwells. Poder et al. [60] found that displacement of heavily weighted catheters, mainly around the urethra, resulted in undertreatment of the central region. Regarding the direction of the error, they stated that errors of 3 mm in the cranial-caudal direction (i.e. longitudinal errors) were more sensitive than the off-axis errors, lateral errors were more sensitive than medial errors, and cranial errors had more impact on the dose plan compared to caudal errors. For off-axis errors, Fichtinger et al. [32] reported a limit of 2 mm, whereas Borghede et al. [29] reported a limit of 3–4 mm, both for LDR BT procedures. For longitudinal errors, limits were reported for HDR BT procedures, ranging from 2 mm [41] to 15 mm [62], whilst most studies reported a limit of 3 mm [35,57,58] or 5 mm [36,43,44,63]. This shows that reported limits for needle positioning errors depend

amongst others on the location of the needle and the direction of the needle positioning error.

4. Discussion

4.1. Main findings

This work provided an overview of the quantification of hazards related to needle positioning in transperineal treatment procedures of localized prostate cancer. We distinguished between the total needle geometry required in the target volume and the individual needle positioning. Firstly, access restrictions to the prostate gland by the pubic arch affect the total needle geometry as the ventrolateral part of the prostate cannot be reached considering the conventional linear trajectories. Obstructions of the prostate up to 22.3 mm were reported for various prostate volumes.

Secondly, individual needle positioning non-conformal to the treatment plan can potentially affect the treatment efficacy. Needle positioning errors were subdivided into mis- and displacement. Needle misplacement was reported for LDR BT, HDR BT, and FLA procedures, in which for LDR BT largest errors were reported, especially in the cranio-caudal direction. Needle displacement was only reported for HDR BT and PDR BT as these techniques involve fractionated doses, whereas LDR BT and FLA are single-dose treatments. Displacements were reported in all directions. The largest displacement was measured in the cranio-caudal direction, and generally increased over time.

Reported clinical guidelines indicate limits regarding prostate volume, PAI, and needle positioning error that, when exceeded, demand for patient exclusion from the procedure or solutions to minimize the impact on the treatment. However, these guidelines are general, ambiguous, and compliance in the clinical setting differs between institutions.

4.2. Limitations

The evaluation of the needle position and the level of PAI depend on (1) patient posture change, (2) imaging modality and specifications, (3) moment of assessment, (4) implemented assessment method, and (5) the assessor. Firstly, patient posture change from supine to lithotomy position introduces discrepancies, and the use of multiple imaging modalities can introduce imaging co-registration inaccuracies [27]. Buus et al. [41] reported that their average MRI-US co-registration error was 0.52 mm with a maximum of 0.95 mm. They stated that organ motion induced by patient posture change affected the outcomes. This is substantiated by Yamoah et al. [64], who revealed that preoperative planning for LDR BT resulted in poorer biochemical control and higher urinary toxicity compared to interventions with intraoperative planning using solely TRUS in lithotomy position.

Secondly, the imaging modality and specifications contribute to uncertainties in the quantitative measurements. CT slice thickness introduces an uncertainty of the needle position because of partial volume artifacts. Kovalchuk et al. [38] considered uncertainty in needle tip determination of 0.63 mm as this was half the slice thickness of their CT slices. Kim et al. [65] reported that an increased CT slice thickness increased the obtained dose error after simulations with random shifting of HDR BT catheters. The mean dose error was 0.7% for 2-mm slices, 1.1% for 3-mm slices, and 1.7% for 5-mm slices. Regarding MRI, Ballester et al. [66] described that the voxel size can change delineation due to blurring [66]. Concerning TRUS, Fedorov *et al.* [67] described that TRUS images have poor contrast at the apex and base of the prostate and can affect the image due to the TRUS probe compressing the prostate gland. Furthermore, ultrasound has a resolution of 200 micrometer, resulting in the lack of tumor visualization because of limited sensitivity [68].

Thirdly, time can be a confounding factor as the observed error depends on the moment of evaluation. Kim et al. [69] described that maximum catheter displacement occurred in the 12 hours after the first fraction for HDR BT, whereas Taschereau et al. [15] reported misplacement of the needles 72 hours after positioning, which makes these measurements potentially to a greater extend subjected to the influence of edema and organ motion.

Fourthly, the assessment method influences the analysis. For example, PAI quantification can be performed by three different methods, and needle positioning errors can be assessed using bone anatomy, metal markers, or other implanted needles as reference markers. Kim et al. [69] reported an average discrepancy of 2.7 mm in needle displacement between measurements using the ischial bone or two gold markers as reference markers.

Lastly, inter-observer variability plays a role in the assessment. Kim et al. [69] reported a difference in displacement error detection of 1.0 ± 0.9 mm with a maximum difference of 5.0 mm between two observers. Therefore, the error threshold should be large enough to be detected, considering all the above-stated inaccuracies, and low enough to avoid a significant impact on the treatment plan.

5. Conclusion

This systematic review of the scientific literature examines the hazards and guidelines associated with needle positioning during transperineal prostate procedures. Current clinical guidelines regarding prostate volume, needle positioning accuracy and maximum allowable PAI are ambiguous, thus a case-specific approach is recommended to avoid a suboptimal procedure or patient exclusion. Steerable needles can offer intraoperative flexibility in needle placement and allow for correction of perturbations while overcoming PAI to ensure an optimized treatment.

6. Expert opinion

6.1. Solution strategies

To operate below the upper limit of the guidelines for needle positioning, countermeasures can be implemented to enable continuation in line with the treatment plan

(Figure 3). Minimizing PAI can be achieved in several ways, subdivided into four pillars: (1) neo-adjuvant hormonal therapy, (2) positioning strategy, (3) needle design, and (4) needle guidance. Improving needle positioning accuracy can be related to (1) positioning strategy and (2) needle design.

Clinical institutions often use hormonal therapy, such as Androgen Deprivation Therapy (ADT), to downsize the prostate gland and reduce the risk of PAI. For example, Kucway et al. [70] showed a volume reduction of the prostate of 33% after 3–4 months of ADT. Traditionally, this therapy is performed prior to the brachytherapy treatment in patients with prostate volumes of 50–60 cc or with observed excessive PAI [22,24,70]. Sejpal et al. [22] reported that 27% of the patients received ADT due to an enlarged prostate or PAI >10 mm. On the other hand, this therapy can induce severe side effects for the patient, such as erectile dysfunction, hot flushes, increased cardiovascular morbidity, and consequently a lower QoL [71–74]. The ABS, therefore, concluded that ADT is only recommended in patients with observed PAI, as no benefit was shown from adding ADT to prostate brachytherapy for low-risk and favorable intermediate-risk patients without PAI [75].

Despite preoperative PAI assessment and the use of ADT in many patients, PAI can still occur during needle implantation. Recently, intraoperative imaging techniques with the patient in the lithotomy position (i.e. needle insertion position), such as intraoperative on-site Cone-Beam CT (CBCT) [76,77] and mobile CT [78] has gained importance in adaptive brachytherapy. Figure 5(a) shows techniques to obtain a conformal total needle geometry if PAI occurs [25]. Regarding positioning strategies, the patient's lithotomy position can be extended, the TRUS probe, the transperineal template or the needle can be manipulated [79], and the needles can be positioned using a free-hand technique without the use of a transperineal template or guide [21,80]. However, the free-hand technique is reported to be difficult and requires experience from the physician, as buckling of the needle can occur due to the absence of the transperineal template for guidance [21]. Concerning needle guidance strategies, the needles can be obliquely positioned using a robotic device for angulated approaches [81], a template sutured to the patient's perineum instead of attached to the TRUS probe, or a patient-specific template [41]. For needle design-related solutions, a needle with an asymmetric tip can be steered using the asymmetric needle-tissue force distribution on the needle tip [55], whereas occasionally the distal tip of a needle is bent in an adequate angle by the physician to circumvent the pubic arch. On the other hand, asymmetric needle tip steering depends on needle-tissue interaction forces making needle control challenging, and a substantial on-site modification in the design of the medical device potentially increases the risk on a needle positioning error. Such designs are referred to as passive steerable needles [82]. De Vries et al. [83] proposed using steerable needles with tip control, known as active steerable needles, to overcome PAI and optimize the dose distribution. Podder et al. [84] described that steerable needles could create curvatures conform the prostate geometry while reducing the total number of needles required, thereby minimizing edema and potentially improving treatment outcomes.

Needle positioning accuracy can be improved by changing the needle design or altering the positioning strategy, as indicated in Figure 5(b). Off-axis errors can be minimized by means of steerable needles that counteract perturbations or robotic devices that minimize insertion or friction forces, thus theoretically reducing needle deflection. Bloemberg et al. [85] described a wasp-inspired, self-propelling, steerable needle that could incorporate an optical fiber for FLA. To reduce longitudinal needle displacement errors, the prostate can be stabilized, the needle can be anchored in the transperineal template sutured to the perineal skin, or the needle design can be adjusted to accomplish needle anchoring once they are inside the prostate [47]. Taschereau et al. [15] used two additional stabilization needles but observed no significant influence on needle displacement. Self-anchoring catheters were described by Pieters et al. [47] and Maenhout et al. [50], with which external fixation in the transperineal template became unnecessary and needle displacement was minimized.

An overarching solution for needle misplacement and displacement errors is repositioning the needles by advancing or retracting them or completely re-implanting them; however, this induces additional tissue trauma [86–88]. In current clinical practice, imaging is often performed after a treatment fraction to evaluate the longitudinal error of the needles, after which displaced needles are advanced again. Keyes et al. [87] described seven patients in which the needles for LDR BT were re-implanted to ensure coverage of the underdosed areas of the prostate. All patients had excellent dosimetry after the re-implantation procedure [87]. Hughes et al. [88] stated that re-implantation increased the prostate dose metrics D90 (i.e. the minimum dose received by 90% of target volume) and V100 (the percentage of the target volume that received at least 100% of the prescription dose [89]) from 49 Gy to 201 Gy and from 46% to 98%, respectively. Noteworthy is the absence of studies related to needle positioning in ablative therapies compared to brachytherapy, which could be explained by the fact that these relatively new ablative therapies are often still in the clinical trial phase [90]. In contrast, brachytherapy has been performed since the early twentieth century [91,92].

Future research should be conducted to better relate hazards of needle positioning in transperineal treatment procedures of localized prostate cancer and clinical outcomes. With this, congruent and adequate guidelines related to PAI and needle positioning error can be implemented. We expect a trend toward novel devices with which challenges in needle positioning can be mitigated, including (1) robotically controlled needles that can be obliquely inserted to improve the accessibility of the target volume while providing very stable and accurate needle guidance [81] and (2) active steerable needles that allow for positioning along curved trajectories to optimize total needle geometry with high positioning

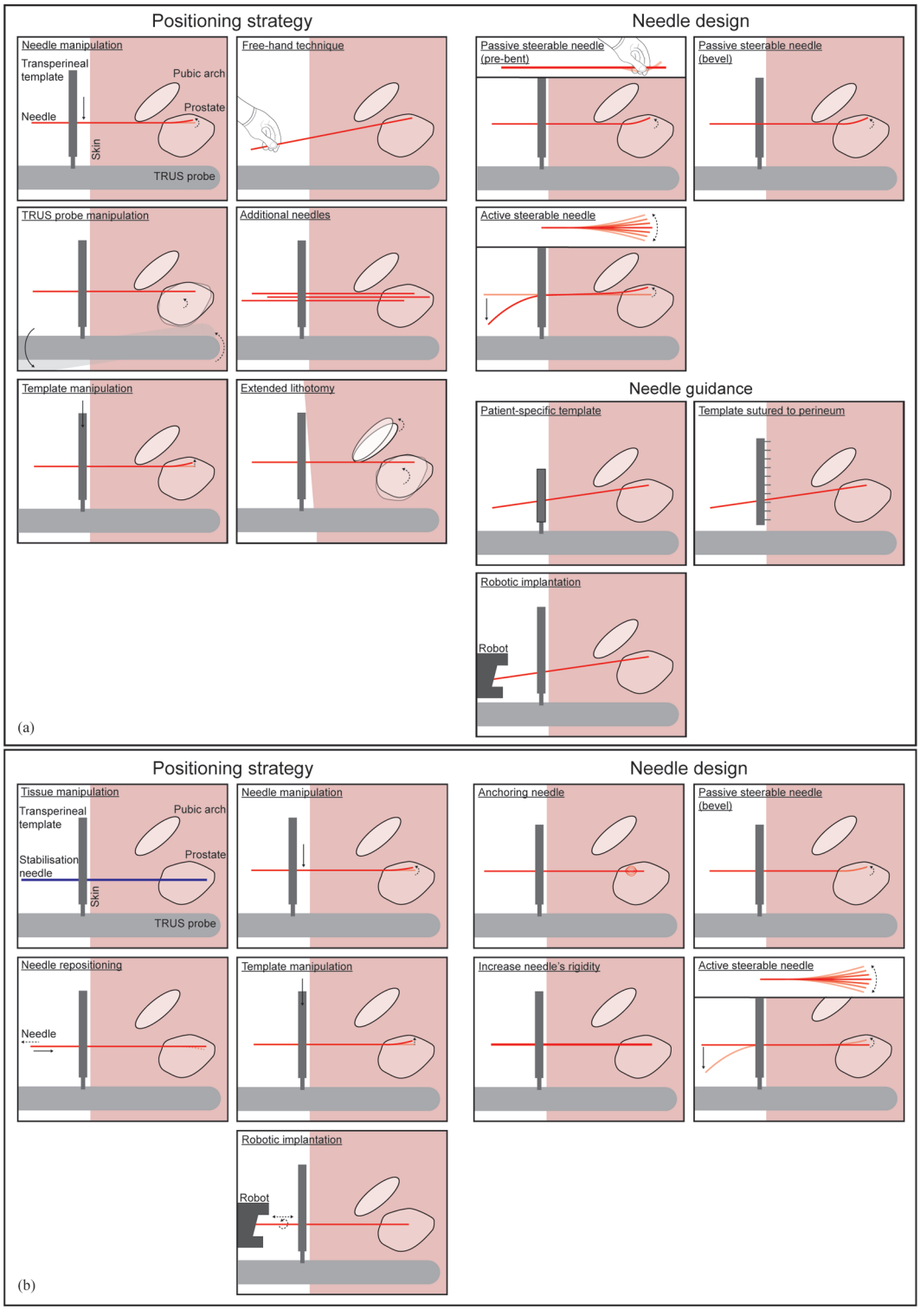

Figure 5. Overview of solution strategies. (a) To improve total needle geometry in prostate with pubic arch interference (PAI), the positioning strategy can be altered by needle manipulation, a free-hand positioning technique, transrectal ultrasound (TRUS) probe manipulation, additional needles, template manipulation, or positioning the patient in the extended lithotomy position. The needle design can be changed by developing a passive steerable needle (e.g. with a pre-bent or a bevel-shaped tip) or an active steerable needle. The needle guidance can be adapted by using a patient-specific template, a template sutured to the patient's perineum instead of attached to the TRUS probe, or robotic implantation of the needle. (b) To improve transperineal needle positioning into the prostate, needle positioning accuracy can be improved by altering the positioning strategy or changing the needle design. The positioning strategy can be altered by tissue manipulation, needle manipulation, needle repositioning, template manipulation, or robotic implantation. The needle design can be changed by developing an anchoring needle, a passive steerable needle (e.g. with a bevel-shaped tip), or an active steerable needle.

accuracy. These solutions should be combined with high-resolution imaging methods like MRI for precise target volume identification and needle guidance. In the scientific literature, steerable needles and brachytherapy robots compatible with MRI are already upcoming; however, these are not common in clinical practice yet [93,94].

Funding

This work was supported by the Netherlands Organisation for Scientific Research [Nederlandse Organisatie voor Wetenschappelijk Onderzoek, NWO], domain Applied and Engineering Sciences (TTW), under Grant 80450; and the European regional development fund under EU Interreg 2 Seas, under Grant: 2S04-022.

Declaration of interest

The authors have no other relevant affiliations or financial involvement with any organization or entity with a financial interest in or financial conflict with the subject matter or materials discussed in the manuscript apart from those disclosed.

Reviewer disclosures

Peer reviewers on this manuscript have no relevant financial relationships or otherwise to disclose.

Acknowledgments

The authors wish to thank Wichor M. Bramer from the Erasmus MC Medical Library for developing and updating the search strategies.

ORCID

Jette Bloemberg http://orcid.org/0000-0002-6627-4165
Luigi A. M. J. G. van Riel http://orcid.org/0000-0001-5759-3909

References

Papers of special note have been highlighted as either of interest (•) or of considerable interest (••) to readers.

1. Sung H, Ferlay J, Siegel RL, et al. Global cancer statistics 2020: GLOBOCAN estimates of incidence and mortality worldwide for 36 cancers in 185 countries. Ca A Cancer J Clin. 2021;71(3):209–249. doi: 10.3322/caac.21660
2. Siegel RL, Miller KD, Wagle NS, et al. Cancer statistics, 2023. CA Cancer J Clin. 2023;73(1):17–48. doi:10.3322/caac.21763
3. Wilt TJ, Brawer MK, Jones KM, et al. Radical prostatectomy versus observation for localized prostate cancer. N Engl J Med. 2012;367(3):203–213. doi: 10.1056/NEJMoa1113162
4. Zhu Z, Zhang J, Liu Y, et al. Efficacy and toxicity of external-beam radiation therapy for localised prostate cancer: a network meta-analysis. Br J Cancer. 2014;110(10):2396–2404. doi:10.1038/bjc.2014.197
5. Martin JM, Handorf EA, Kutikov A, et al. The rise and fall of prostate brachytherapy: use of brachytherapy for the treatment of localized prostate cancer in the national cancer data base. Cancer. 2014;120(14):2114–2121. doi: 10.1002/cncr.28697
6. Jain A, Deguet A, Iordachita I, et al. Intra-operative 3D guidance and edema detection in prostate brachytherapy using a non-isocentric C-arm. Med Image Anal. 2012;16(3):731–743. doi: 10.1016/j.media.2010.07.011
7. Frank SJ, Pisters LL, Davis J, et al. An assessment of quality of life following radical prostatectomy, high dose external beam radiation therapy and brachytherapy iodine implantation as monotherapies for localized prostate cancer. J Urol. 2007;177(6):2151–2156. doi:10.1016/j.juro.2007.01.134
8. Lodeizen O, de Bruin M, Eggener S, et al. Ablation energies for focal treatment of prostate cancer. World J Urol. 2019;37(3):409–418. doi: 10.1007/s00345-018-2364-x
9. De La Rosette J, Ahmed H, Barentsz J, et al. Focal therapy in prostate cancer—report from a consensus panel. Jf Endourol. 2010;24(5):775–780. doi: 10.1089/end.2009.0596
10. Tincher SA, Kim RY, Ezekiel MP, et al. Effects of pelvic rotation and needle angle on pubic arch interference during transperineal prostate implants. Int J Radiat Oncol Biol Phys. 2000;47(2):361–363. doi: 10.1016/S0360-3016(00)00434-X
11. Mate TP, Gottesman JE, Hatton J, et al. High dose-rate afterloading 192Iridium prostate brachytherapy: feasibility report. Int J Radiat Oncol Biol Phys. 1998;41(3):525–533. doi: 10.1016/S0360-3016(98)00097-2
12. Whiting P, Rutjes AW, Reitsma JB, et al. The development of QUADAS: a tool for the quality assessment of studies of diagnostic accuracy included in systematic reviews. BMC Med Res Methodol. 2003;3(1):1–13. doi: 10.1186/1471-2288-3-25
13. D'Souza D, Baldassarre F, Morton G, et al. Imaging technologies for high dose rate brachytherapy for cervical cancer: a systematic review. Clin Oncol. 2011;23(7):460–475. doi:10.1016/j.clon.2011.02.014
14. Jamema SV, Saju S, Shetty UM, et al. Dosimetric comparison of inverse optimization with geometric optimization in combination with graphical optimization for HDR prostate implants. J Med Phys/Assoc Med Physicists India. 2006;31(2):89. doi: 10.4103/0971-6203.26694
15. Taschereau R, Pouliot J, Roy J, et al. Seed misplacement and stabilizing needles in transperineal permanent prostate implants. Radiother Oncol. 2000;55(1):59–63. doi: 10.1016/S0167-8140(00)00162-6
16. de Vries M, Wilby S, Palmer AL, et al. Overcoming pubic arch interference in prostate brachytherapy using steerable needles. J Contemp Brachytherapy. 2022;14(5):495–500. doi: 10.5114/jcb.2022.121562
17. Zheng Y, Wu J, Chen S, et al. Predicting pubic arch interference in permanent prostate brachytherapy based on the specific parameters derived from nuclear magnetic resonance imaging. J Contemp Brachytherapy. 2018;10(5):405–410. doi: 10.5114/jcb.2018.79247
18. Martin GV, Pugh TJ, Mahmood U, et al. Permanent prostate brachytherapy pubic arch evaluation with diagnostic magnetic resonance imaging. Brachytherapy. 2017;16(4):728–733. doi: 10.1016/j.brachy.2017.02.001
19. Fukada J, Shigematsu N, Nakashima J, et al. Predicting pubic arch interference in prostate brachytherapy on transrectal ultrasonography-computed tomography fusion images. J Radiat Res. 2012;53(5):753–759. doi: 10.1093/jrr/rrs020
20. Ryu B, Bax J, Edirisinge C, et al. Prostate brachytherapy with oblique needles to treat large glands and overcome pubic arch interference. Int J Radiat Oncol Biol Phys. 2012;83:1463–1472. doi: 10.1016/j.ijrobp.2011.10.012
21. Gibbons EP, Smith RP, Beriwal S, et al. Overcoming pubic arch interference with free-hand needle placement in men undergoing prostate brachytherapy. Brachytherapy. 2009;8(1):74–78. doi: 10.1016/j.brachy.2008.04.007
22. Sejpal SV, Sathiaseelan V, Helenowski IB, et al. Intra-operative pubic arch interference during prostate seed brachytherapy in patients with CT-based pubic arch interference of ≤1 cm. Radiother Oncol. 2009;91(2):249–254. doi: 10.1016/j.radonc.2009.02.006
• **Large study (n = 243) showing pubic arch interference during brachytherapy.**
23. Nickers P, Thissen B, Jansen N, et al. 192Ir or 125I prostate brachytherapy as a boost to external beam radiotherapy in locally advanced prostatic cancer: a dosimetric point of view. Radiother Oncol. 2006;78(1):47–52. doi: 10.1016/j.radonc.2005.09.002
24. Henderson A, Laing RW, Langley SEM. Identification of pubic arch interference in prostate brachytherapy: simplifying the transrectal ultrasound technique. Brachytherapy. 2003;2(4):240–245. doi: 10.1016/j.brachy.2003.11.001

25. Strang JG, Rubens DJ, Brasacchio RA, et al. Real-time US versus CT determination of pubic arch interference for brachytherapy. Radiology. 2001;219(2):387–393. doi: 10.1148/radiology.219.2.r01ma37387
26. Wang H, Wallner K, Sutlief S, et al. Transperineal brachytherapy in patients with large prostate glands. Int J Cancer. 2000;90(4):199–205. doi: 10.1002/1097-0215(20000820)90:4<199:AID-IJC3>3.0.CO;2-C
27. Bellon J, Wallner K, Ellis W, et al. Use of pelvic CT scanning to evaluate pubic arch interference of transperineal prostate brachytherapy. Int J Radiat Oncol Biol Phys. 1999;43(3):579–581. doi: 10.1016/S0360-3016(98)00466-0
28. Wallner K, Ellis W, Russell K, et al. Use of TRUS to predict pubic arch interference of prostate brachytherapy. Int J Radiat Oncol Biol Phys. 1999;43:583–585. doi: 10.1016/S0360-3016(98)00459-3
29. Borghede G, Hedelin H, Holmäng S, et al. Irradiation of localized prostatic carcinoma with a combination of high dose rate iridium-192 brachytherapy and external beam radiotherapy with three target definitions and dose levels inside the prostate gland. Radiother Oncol. 1997;44:245–250. doi: 10.1016/S0167-8140(97)00122-9
30. Jamaluddin MF, Ghosh S, Waine MP, et al. Quantifying 125I placement accuracy in prostate brachytherapy using postimplant transrectal ultrasound images. Brachytherapy. 2017;16(2):306–312. doi: 10.1016/j.brachy.2016.11.015
31. Cepek J, Lindner U, Ghai S, et al. Mechatronic system for in-bore MRI-guided insertion of needles to the prostate: an in vivo needle guidance accuracy study. J Magn Reson Imaging. 2015;42(1):48–55. doi: 10.1002/jmri.24742
32. Fichtinger G, Fiene JP, Kennedy CW, et al. Robotic assistance for ultrasound-guided prostate brachytherapy. Med Image Anal. 2008;12:535–545. doi: 10.1016/j.media.2008.06.002
33. Szlag M, Ślosarek K, Rembielak A, et al. Real-time brachytherapy for prostate cancer – implant analysis. Rep Pract Oncol Radiother. 2008;13(1):9–14. doi: 10.1016/S1507-1367(10)60076-4
34. Cormack RA, Tempany CM, D'Amico AV. Optimizing target coverage by dosimetric feedback during prostate brachytherapy. Int J Radiat Oncol Biol Phys. 2000;48(4):1245–1249. doi: 10.1016/S0360-3016(00)00742-2
35. Huang Y, Miller B, Doemer A, et al. Online correction of catheter movement using CT in high-dose-rate prostate brachytherapy. Brachytherapy. 2013;12(3):260–266. doi: 10.1016/j.brachy.2012.08.008
36. Whitaker M, Hruby G, Lovett A, et al. Prostate HDR brachytherapy catheter displacement between planning and treatment delivery. Radiother Oncol. 2011;101:490–494. doi: 10.1016/j.radonc.2011.08.004
37. Holly R, Morton GC, Sankreacha R, et al. Use of cone-beam imaging to correct for catheter displacement in high dose-rate prostate brachytherapy. Brachytherapy. 2011;10(4):299–305. doi: 10.1016/j.brachy.2010.11.007
38. Kovalchuk N, Furutani KM, MacDonald OK, et al. Dosimetric effect of interfractional needle displacement in prostate high-dose-rate brachytherapy. Brachytherapy. 2012;11(2):111–118. doi: 10.1016/j.brachy.2011.05.006
39. Reynés-Llompart G, Pino F, Modolell I, et al. Impact of prostate catheter displacement in inverse planning–simulated annealing and geometric optimization. Brachytherapy. 2016;15(1):112–117. doi: 10.1016/j.brachy.2015.10.003
40. Carrara M, Tenconi C, Mazzeo D, et al. Study of the correlation between rectal wall in vivo dosimetry performed with MOSkins and implant modification during TRUS-guided HDR prostate brachytherapy. Radiat Meas. 2017;106:385–390. doi: 10.1016/j.radmeas.2017.03.016
41. Buus S, Lizondo M, Hokland S, et al. Needle migration and dosimetric impact in high-dose-rate brachytherapy for prostate cancer evaluated by repeated MRI. Brachytherapy. 2018;17(1):50–58. doi: 10.1016/j.brachy.2017.08.005
42. Mullokandov E, Gejerman G. Analysis of serial CT scans to assess template and catheter movement in prostate HDR brachytherapy. Int J Radiat Oncol Biol Phys. 2004;58(4):1063–1071. doi: 10.1016/j.ijrobp.2003.08.020
43. Damore SJ, Syed AMN, Puthawala AA, et al. Needle displacement during HDR brachytherapy in the treatment of prostate cancer. Int J Radiat Oncol Biol Phys. 2000;46(5):1205–1211. doi: 10.1016/S0360-3016(99)00477-0
44. Pellizzon ACA, Salvajoli JV, Novaes PERS, et al. Needle displacement during high-dose-rate afterloading brachytherapy boost and conventional external beam radiation therapy for initial and local advanced prostate cancer. Urol Int. 2003;70(3):200–204. doi: 10.1159/000068775
45. Smith RL, Hanlon M, Panettieri V, et al. An integrated system for clinical treatment verification of HDR prostate brachytherapy combining source tracking with pretreatment imaging. Brachytherapy. 2018;17(1):111–121. doi: 10.1016/j.brachy.2017.08.004
46. Martinez AA, Pataki I, Edmundson G, et al. Phase II prospective study of the use of conformal high-dose-rate brachytherapy as monotherapy for the treatment of favorable stage prostate cancer: a feasibility report. Int J Radiat Oncol Biol Phys. 2001;49(1):61–69. doi: 10.1016/S0360-3016(00)01463-2
47. Pieters BR, van der Grient JNB, Blank LECM, et al. Minimal displacement of novel self-anchoring catheters suitable for temporary prostate implants. Radiother Oncol. 2006;80(1):69–72. doi: 10.1016/j.radonc.2006.06.014
    •• **Describes unique PDR BT catheters with an umbrella anchoring mechanism at the tip to fixate the catheter inside the prostate gland.**
48. Fox CD, Kron T, Leahy M, et al. Interfraction patient motion and implant displacement in prostate high dose rate brachytherapy. Med Phys. 2011;38(11):5838–5843. doi: 10.1118/1.3641865
49. Hoskin PJ, Bownes PJ, Ostler P, et al. High dose rate afterloading brachytherapy for prostate cancer: catheter and gland movement between fractions. Radiother Oncol. 2003;68(3):285–288. doi: 10.1016/S0167-8140(03)00203-2
50. Maenhout M, van der Voort van Zyp JRN, Borot de Battisti M, et al. The effect of catheter displacement and anatomical variations on the dose distribution in MRI-guided focal HDR brachytherapy for prostate cancer. Brachytherapy. 2018;17(1):24–30. doi: 10.1016/j.brachy.2017.04.239
51. Dickhoff LR, Kerkhof EM, Deuzeman HH, et al. Adaptive objective configuration in bi-objective evolutionary optimization for cervical cancer brachytherapy treatment planning. Proceedings of the Genetic and Evolutionary Computation Conference; 2022;1173–1181.
52. Davis BJ, Horwitz EM, Lee WR, et al. American brachytherapy society consensus guidelines for transrectal ultrasound-guided permanent prostate brachytherapy. Brachytherapy. 2012;11(1):6–19. doi: 10.1016/j.brachy.2011.07.005
53. Henry A, Pieters BR, Siebert FA, et al. GEC-ESTRO ACROP prostate brachytherapy guidelines. Radiother Oncol. 2022;167:244–251. doi:10.1016/j.radonc.2021.12.047
54. van Gerwen DJ, Dankelman J, van den Dobbelsteen JJ. Needle–tissue interaction forces–a survey of experimental data. Med Eng & Phys. 2012;34(6):665–680. doi: 10.1016/j.medengphy.2012.04.007
55. Misra S, Reed KB, Douglas AS, et al. Needle-tissue interaction forces for bevel-tip steerable needles. In: 2008 2nd IEEE RAS & EMBS International Conference on Biomedical Robotics and Biomechatronics; Scottsdale, AZ, USA. IEEE; 2008. p. 224–231.
    • **Describes model for needle-tissue interaction forces for steerable needles.**
56. Wan G, Wei Z, Gardi L, et al. Brachytherapy needle deflection evaluation and correction. Med Phys. 2005;32:902–909. doi: 10.1118/1.1871372
57. Aluwini S, Busser WMH, Baartman LEA, et al. Fractionated high-dose-rate brachytherapy as monotherapy in prostate cancer: does implant displacement and its correction influence acute and late toxicity? Brachytherapy. 2016;15(6):707–713. doi: 10.1016/j.brachy.2016.05.008

58. Tiong A, Bydder S, Ebert M, et al. A small tolerance for catheter displacement in high–dose rate prostate brachytherapy is necessary and feasible. Int J Radiat Oncol Biol Phys. 2010;76(4):1066–1072. doi: 10.1016/j.ijrobp.2009.03.052
59. Kolkman-Deurloo IKK, Roos MA, Aluwini S. HDR monotherapy for prostate cancer: a simulation study to determine the effect of catheter displacement on target coverage and normal tissue irradiation. Radiother Oncol. 2011;98:192–197. doi: 10.1016/j.radonc.2010.12.009
60. Poder J, Carrara M, Howie A, et al. Derivation of in vivo source tracking error thresholds for TRUS-based HDR prostate brachytherapy through simulation of source positioning errors. Brachytherapy. 2019;18(5):711–719. doi: 10.1016/j.brachy.2019.05.001
61. Mason J, Henry A, Bownes P. Error detection thresholds for routine real time in vivo dosimetry in HDR prostate brachytherapy. Radiother Oncol. 2020;149:38–43. doi:10.1016/j.radonc.2020.04.058
62. Takenaka T, Yoshida K, Ueda M, et al. Assessment of daily needle applicator displacement during high-dose-rate interstitial brachytherapy for prostate cancer using daily CT examinations. J RAD Res. 2012;53:469–474. doi: 10.1269/jrr.11168
63. Simnor T, Li S, Lowe G, et al. Justification for inter-fraction correction of catheter movement in fractionated high dose-rate brachytherapy treatment of prostate cancer. Radiother Oncol. 2009;93(2):253–258. doi: 10.1016/j.radonc.2009.09.015
64. Yamoah K, Eldredge-Hindy HB, Zaorsky NG, et al. Large prostate gland size is not a contraindication to low-dose-rate brachytherapy for prostate adenocarcinoma. Brachytherapy. 2014;13(5):456–464. doi: 10.1016/j.brachy.2014.04.003
65. Kim Y, Hsu IC, Lessard E, et al. Dosimetric impact of prostate volume change between CT-based HDR brachytherapy fractions. Int J Radiat Oncol Biol Phys. 2004;59(4):1208–1216. doi: 10.1016/j.ijrobp.2004.02.053
66. Ballester MAG, Zisserman AP, Brady M. Estimation of the partial volume effect in MRI. Med Image Anal. 2002;6(4):389–405. doi: 10.1016/S1361-8415(02)00061-0
67. Fedorov A, Khallaghi S, Sánchez CA, et al. Open-source image registration for MRI–TRUS fusion-guided prostate interventions. Int J Comput Assist Radiol Surg. 2015;10(6):925–934. doi: 10.1007/s11548-015-1180-7
68. Klotz CL. Can high resolution micro-ultrasound replace MRI in the diagnosis of prostate cancer? Eur Urol Focus. 2020;6(2):419–423. doi: 10.1016/j.euf.2019.11.006
69. Kim Y, Hsu IC, Pouliot J. Measurement of craniocaudal catheter displacement between fractions in computed tomography–based high dose rate brachytherapy of prostate cancer. J Appl Clin Med Phys. 2007;8(4):1–13. doi: 10.1120/jacmp.v8i4.2415
70. Kucway R, Vicini F, Huang R, et al. Prostate volume reduction with androgen deprivation therapy before interstitial brachytherapy. J Urol. 2002;167(6):2443–2447. doi: 10.1016/S0022-5347(05)65001-X
71. Press RH, Morgan TM, Cutrell PK, et al. Patient-reported health-related quality of life outcomes after HDR brachytherapy between small (<60 cc) and large (≥60 cc) prostate glands. Brachytherapy. 2019;18:13–21. doi: 10.1016/j.brachy.2018.08.009
72. Kopp RP, Marshall LM, Wang PY, et al. The burden of urinary incontinence and urinary bother among elderly prostate cancer survivors. Eur Urol. 2013;64(4):672–679. doi: 10.1016/j.eururo.2013.03.041
73. Saigal CS, Gore JL, Krupski TL, et al. Androgen deprivation therapy increases cardiovascular morbidity in men with prostate cancer. Cancer: Interdiscip Int J Am Cancer Soc. 2007;110(7):1493–1500. doi:10.1002/cncr.22933
74. Basaria S, Lieb J, Tang AM, et al. Long-term effects of androgen deprivation therapy in prostate cancer patients. Clinical Endocrinol. 2002;56(6):779–786. doi: 10.1046/j.1365-2265.2002.01551.x
75. Keyes M, Merrick G, Frank SJ, et al. Use of androgen deprivation therapy with prostate brachytherapy, a systematic literature review. Brachytherapy. 2017;16(2):245. doi: 10.1016/j.brachy.2016.11.017
76. Karius A, Strnad V, Lotter M, et al. First clinical experience with a novel, mobile cone-beam CT system for treatment quality assurance in brachytherapy. Strahlenther Onkol. 2022;198(6):573–581. doi: 10.1007/s00066-022-01912-7
77. Karius A, Karolczak M, Strnad V, et al. Technical evaluation of the cone-beam computed tomography imaging performance of a novel, mobile, gantry-based X-ray system for brachytherapy. J Appl Clin Med Phys. 2022;23(2):e13501. doi: 10.1002/acm2.13501
78. Chernavsky NE, Morcos M, Wu P, et al. Technical assessment of a mobile CT scanner for image-guided brachytherapy. J Appl Clin Med Phys. 2019;20(10):187–200. doi: 10.1002/acm2.12738
79. Stone NN, Stock RG. Prostate brachytherapy in patients with prostate volumes ≥ 50 cm3: dosimetic analysis of implant quality. Int J Radiat Oncol Biol Phys. 2000;46:1199–1204. doi: 10.1016/S0360-3016(99)00516-7
80. Roy JN, Wallner KE, Chiu-Tsao ST, et al. CT-based optimized planning for transperineal prostate implant with customized template. Int J Radiat Oncol Biol Phys. 1991;21(2):483–489. doi: 10.1016/0360-3016(91)90800-J
81. Kettenbach J, Kronreif G. Robotic systems for percutaneous needle-guided interventions. Minimally Invasive Ther Allied Technol. 2015;24(1):45–53. doi:10.3109/13645706.2014.977299
82. van de Berg NJ, Dankelman J, van den Dobbelsteen JJ. Design of an actively controlled steerable needle with tendon actuation and FBG-based shape sensing. Med Eng Phys. 2015;37(6):617–622. doi: 10.1016/j.medengphy.2015.03.016
83. de Vries M, Sikorski J, Misra S, et al. Axially rigid steerable needle with compliant active tip control. PLOS ONE. 2021;16(12):e0261089. doi:10.1371/journal.pone.0261089
84. Podder TK, Dicker AP, Hutapea P, et al. A novel curvilinear approach for prostate seed implantation. Med Phys. 2012;39(4):1887–1892. doi: 10.1118/1.3694110

•• **Describes needles that could create curvatures conform the prostate geometry while reducing the total number of needles required, thereby minimizing oedema and potentially improving treatment outcome.**

85. Bloemberg J, Trauzettel F, Coolen B, et al. Design and evaluation of an MRI-ready, self-propelled needle for prostate interventions. PLOS ONE. 2022;17(9):e0274063. doi:10.1371/journal.pone.0274063
86. Marcu LG, Lawson JM. Technical and dosimetric aspects of iodine-125 seed reimplantation in suboptimal prostate implants. Br J Radiol. 2013;86(1026):20130058. doi: 10.1259/bjr.20130058
87. Keyes M, Pickles T, Agranovich A, et al. 125I reimplantation in patients with poor initial dosimetry after prostate brachytherapy. Int J Radiat Oncol Biol Phys. 2004;60(1):40–50. doi: 10.1016/j.ijrobp.2004.02.011
88. Hughes L, Waterman FM, Dicker AP. Salvage of suboptimal prostate seed implantation: reimplantation of underdosed region of prostate base. Brachytherapy. 2005;4(2):163–170. doi: 10.1016/j.brachy.2005.03.002
89. Morris WJ, Spadinger I, Keyes M, et al. Whole prostate D90 and V100: a dose–response analysis of 2000 consecutive 125I monotherapy patients. Brachytherapy. 2014;13(1):32–41. doi: 10.1016/j.brachy.2013.08.006
90. Natarajan S, Raman S, Priester AM, et al. Focal laser ablation of prostate cancer: phase I clinical trial. J Urol. 2016;196:68–75. doi: 10.1016/j.juro.2015.12.083
91. Skowronek J. Current status of brachytherapy in cancer treatment–short overview. J Contemp Brachytherapy. 2017;9(6):581–589. doi: 10.5114/jcb.2017.72607
92. Devlin PM, Holloway CL, Stewart AJ. Brachytherapy: applications and techniques. New York: Springer Publishing Company; 2015.
93. Fischer GS, Iordachita I, Csoma C, et al. MRI-compatible pneumatic robot for transperineal prostate needle placement. IEEE/ASME Trans Mechatron. 2008;13(3):295–305. doi: 10.1109/TMECH.2008.924044
94. Siepel FJ, Maris B, Welleweerd MK, et al. Needle and biopsy robots: a review. Curr Robot Rep. 2021;2(1):73–84. doi: 10.1007/s43154-020-00042-1
95. David A, Brennan V, Cohen G, et al. Is there a clinically meaningful change in anatomy during planning of US HDR prostate brachytherapy? Radiother Oncol. 2019;133:S586. doi: 10.1016/S0167-8140(19)31472-0

96. Wu CHD, Thind K, Husain S, et al. 63 prostate and catheter motion in prostate HDR brachytherapy: from operating room to shielded delivery vault. Radiother Oncol. 2019;139:S29. doi:10.1016/S0167-8140(19)33352-3
97. Peddada AV, Blasi OC, White GA, et al. Prevention of needle displacement in multifraction high-dose-rate prostate brachytherapy: a prospective volumetric analysis and technical considerations. Pract Radiat Oncol. 2015;5:228–237. doi: 10.1016/j.prro.2014.11.004
98. Dinkla AM, Pieters BR, Koedooder K, et al. Prostate volume and implant configuration during 48 hours of temporary prostate brachytherapy: limited effect of oedema. Radiat Oncol. 2014;9. doi: 10.1186/s13014-014-0272-9
99. Kawakami S, Ishiyama H, Terazaki T, et al. Catheter displacement prior to the delivery of high-dose-rate brachytherapy in the treatment of prostate cancer patients. J Contemp Brachytherapy. 2014;6:161–166. doi: 10.5114/jcb.2014.43619
100. Foster W, Cunha JAM, Hsu IC, et al. Dosimetric impact of interfraction catheter movement in high-dose rate prostate brachytherapy. Int J Radiat Oncol Biol Phys. 2011;80:85–90. doi: 10.1016/j.ijrobp.2010.01.016
101. Milickovic N, Mavroidis P, Tselis N, et al. 4D analysis of influence of patient movement and anatomy alteration on the quality of 3D U/S-based prostate HDR brachytherapy treatment delivery. Med Phys. 2011;38(9):4982–4993. doi: 10.1118/1.3618735
102. Yoshida K, Yamazaki H, Nose T, et al. Needle applicator displacement during high-dose-rate interstitial brachytherapy for prostate cancer. Brachytherapy. 2010;9(1):36–41. doi: 10.1016/j.brachy.2009.04.006